BRAIN
A JOURNAL OF NEUROLOGY

Electroencephalographic source imaging: a prospective study of 152 operated epileptic patients

Verena Brodbeck,[1] Laurent Spinelli,[2] Agustina M. Lascano,[1] Michael Wissmeier,[3] Maria-Isabel Vargas,[3] Serge Vulliemoz,[2] Claudio Pollo,[4] Karl Schaller,[5] Christoph M. Michel[1] and Margitta Seeck[2]

1 Department of Basic and Clinical Neurosciences, University of Geneva, 1211 Geneva, Switzerland
2 EEG and Epilepsy Unit, Neurology Clinic, University Hospital Geneva, 1211 Geneva, Switzerland
3 Department of Radiology, University Hospital of Geneva, 1211 Geneva, Switzerland
4 Department of Neurosurgery, University Hospital (CHUV), 1011 Lausanne, Switzerland
5 Department of Neurosurgery, University Hospital Geneva, 1211 Geneva, Switzerland

Correspondence to: Prof. Margitta Seeck, MD,
EEG and Epilepsy Unit, Neurology Clinic,
University Hospital (HUG) and University of Geneva,
4, Rue Gabrielle-Perret-Gentil,
CH-1211, Geneva
E-mail: margitta.seeck@hcuge.ch

Electroencephalography is mandatory to determine the epilepsy syndrome. However, for the precise localization of the irritative zone in patients with focal epilepsy, costly and sometimes cumbersome imaging techniques are used. Recent small studies using electric source imaging suggest that electroencephalography itself could be used to localize the focus. However, a large prospective validation study is missing. This study presents a cohort of 152 operated patients where electric source imaging was applied as part of the pre-surgical work-up allowing a comparison with the results from other methods. Patients (n = 152) with >1 year postoperative follow-up were studied prospectively. The sensitivity and specificity of each imaging method was defined by comparing the localization of the source maximum with the resected zone and surgical outcome. Electric source imaging had a sensitivity of 84% and a specificity of 88% if the electroencephalogram was recorded with a large number of electrodes (128–256 channels) and the individual magnetic resonance image was used as head model. These values compared favourably with those of structural magnetic resonance imaging (76% sensitivity, 53% specificity), positron emission tomography (69% sensitivity, 44% specificity) and ictal/interictal single-photon emission-computed tomography (58% sensitivity, 47% specificity). The sensitivity and specificity of electric source imaging decreased to 57% and 59%, respectively, with low number of electrodes (<32 channels) and a template head model. This study demonstrated the validity and clinical utility of electric source imaging in a large prospective study. Given the low cost and high flexibility of electroencephalographic systems even with high channel counts, we conclude that electric source imaging is a highly valuable tool in pre-surgical epilepsy evaluation.

Introduction

Surgical resection of the epileptogenic zone is an under-utilized and potentially curative treatment for pharmacoresistant patients with focal epilepsy. Crucial to the success of surgical treatment is a robust pre-surgical evaluation protocol that identifies and localizes the epileptic focus—both to specify the surgical target and to define that target's proximity to indispensable cortical areas. Non-invasive imaging methods are of utmost importance in the pre-surgical evaluation process. In clear cases, they make further invasive investigations—with their inevitable costs and risks— unnecessary. In more difficult cases, they give important *a priori* information that guides and helps validate the results of the invasive procedures.

So what methods should this non-invasive pre-surgical protocol include? Magnetic resonance imaging (MRI), positron emission tomography (PET) and single-photon emission-computerized tomography (SPECT) are the most established non-invasive imaging methods in pre-surgical evaluation and have their undoubted value. They correctly localize the epileptic area in ~50–80% of cases depending on the presence or absence of a structural lesion (Spanaki *et al.*, 1999; Henry and van Heertum, 2003; Knowlton *et al.*, 2008). The conventional 19- to 32-scalp EEG is generally not considered a reliable localization method, even though it is the most essential tool to characterize the epileptic syndrome.

A recent comprehensive review (Plummer *et al.*, 2008) suggests that electric source imaging deserves a place in the routine work-up of patients with localization-related epilepsy. Electric source imaging is a technique that applies inverse source estimation methods to non-invasive scalp EEG recorded with multiple electrodes arrayed across the entire scalp ('whole head'). However, the authors noted that while studies done to date— largely with small patient numbers—were promising, a prospective validation study conducted on a larger patient group was still required. With the present study, we intend to fill that gap. We report the results of a prospective and blinded electric source imaging analysis of 152 patients who were subsequently operated with a follow-up period of >1 year.

One point that deserves special attention relates to the usefulness of the non-invasive methods for surgical guidance. Electric source imaging is the co-registration of the electric source estimations with the brain structure of the individual patient or a template MRI. Many of the source localization studies in epilepsy [particularly those using magnetoencephalography (MEG)] utilize spherical head models and subsequent co-registration of equivalent dipoles with the patient's MRI using simple fiducial-based matching methods (e.g. Sutherling *et al.*, 2008; Knowlton *et al.*, 2009). Others utilize a template MRI to construct a realistic head model based on finite or boundary element meshing methods (Fuchs *et al.*, 2006; Zumsteg *et al.*, 2006; Holmes *et al.*, 2008; Wennberg *et al.*, 2011). From a surgical point of view, it is obvious that such strategies do not necessarily provide correct solutions within the 'individual' patient brain on which the surgeon wants to operate. Particularly, lesions and deformations are not taken into account despite the fact that brain anomalies are often encountered in symptomatic epilepsy.

While the advantages of using the individual brain as head model for source localization are obvious, a study showing the effective benefit as compared with a template brain in a large patient cohort has not yet been performed. Likewise, the benefit of large electrode arrays as compared with the conventional clinical EEG with low number of electrodes has also not been completely settled.

The specific goals of our study were therefore to: (i) determine the sensitivity and specificity of electric source imaging using standard clinical recordings with fewer than 30 electrodes versus a high number of electrodes (128–256 electrodes); (ii) to analyse the benefit of using individual MRI as a head model for accurate source localization; and (iii) to compare electric source imaging with other established imaging tools including MRI, PET and SPECT.

Materials and methods

Patients

For this study, we included patients from our database matching the following inclusion criteria: they (i) suffered from pharmacoresistant focal epilepsy; (ii) underwent pre-surgical evaluation with MRI and long-term video-EEG recording; (iii) underwent surgical resection of the presumed epileptogenic zone; and (iv) had a post-surgical follow-up of at least 12 months.

We included in this series all 152 patients (76 male) who matched the inclusion criteria. The age range at the time of the surgical intervention was 1–60 years (median 26.6; mean 26.8 years). The age range at epilepsy onset was 0 (post-natal) to 54 years (median 8.0; mean 11.2 years). Site of surgery was temporal ($n = 102$) or extratemporal ($n = 50$; Table 1). Outcome was good to excellent (i.e. Classes 1 and 2) in 88% of all the patients (Table 2). Outcome differed between both groups, with better results in the patients with temporal lobe epilepsy, compared with the patients with extratemporal lobe epilepsy ($P < 0.01$; Table 2). Twenty-nine patients had a Phase II investigation with intracranial recordings. Supplementary Table 1 gives the characteristics of each of the 152 patients.

Table 1 Site of surgery ($n = 152$)

Site of surgery	n
Temporal lobe surgery	102
Extratemporal lobe surgery	50
Single lobe	
Frontal	18
Parietal	6
Occipital	5
Multiple lobes	
Temporo-parietal	6
Parieto-occipital	4
Fronto-temporal	3
Temporo-occipital	2
Fronto-central	1
Temporo-parieto-occiptal	4
Fronto-parieto-temporal	1

Table 2 Outcome after surgery

Group	Engel Class I (%)	Engel Class II (%)	Engel Class III (%)	Engel Class IV (%)
All (n = 152)	117 (77.0)	16 (10.5)	13 (8.6)	6 (4.0)
Temporal (n = 102)	87 (85.3)	9 (8.8)	2 (2.0)	4 (3.9)
Extratemporal (n = 50)	30 (60.0)	7 (14.0)	11 (22.0)	2 (4.0)

Engel Class I: no more seizures with impaired consciousness; Class II: decrease of seizures of >80%; Class III: decrease of 50–80%; Class IV: decrease <50%. Difference between the outcome of temporal and extratemporal lobe surgery is significant ($P < 0.01$).
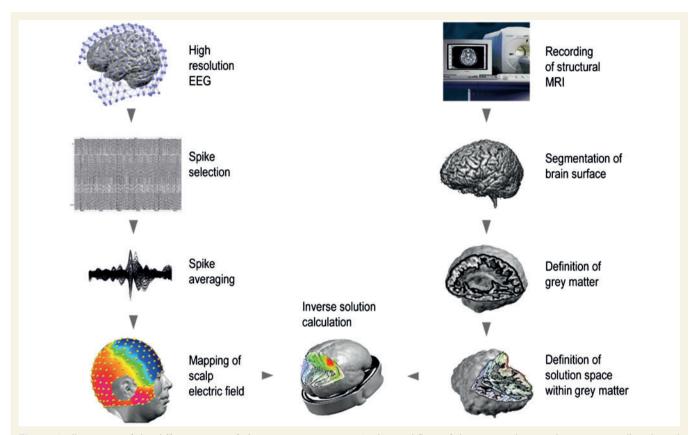

Figure 1 Illustration of the different steps of electric source imaging. (*Left*) Workflow of the EEG analysis. Spikes are manually selected from the EEG (here: 256 channels) and averaged. The potential map at 50% of the rising phase of the averaged spike is used for source analysis. (*Right*) Workflow of the automatic MRI analysis. Segmentation of the brain and grey matter allowed building a simplified realistic head model (SMAC model) with the solution points distributed in the grey matter of the individual brain. This head model is used for the inverse solution calculation, which in this study was based on a distributed linear inverse solution called LAURA.

Electroencephalogram recordings

Conventional long-term video-EEG recording was performed on all patients with standard clinical EEG setups of 19–29 electrodes (10/10 system). Impedances were kept below 10 kΩ, the sampling rate was 256 Hz and band-pass filters were set to 0.1 and 120 Hz, with a vertex contact as the reference electrode.

Ictal scalp recordings were obtained in our laboratory in 146 patients. They were of frontal origin in 12, temporal in 81, parietal in two and occipital in five patients. Seven patients had non-localizing ictal discharges and 35 had bilateral onset.

In 55 patients, a high-resolution EEG was also recorded. Of these patients, 14 had 256 electrode array recordings and 40 had recordings with 128 electrode arrays. For one young patient (2 years old),

a 64 electrode array was used. The high-resolution EEG was recorded with the Geodesic Sensor Net® where the electrodes are interconnected by thin rubber bands, containing small sponges soaked with saline water that touch the patient's scalp surface directly (Electrical Geodesics Inc.). The net was adjusted so that Fpz, Cz, Oz and the pre-auricular points were correctly placed according to the international 10/10 system. The tension structure of the net ensured that the electrodes were evenly distributed over the scalp and that they were positioned at approximately the same location across patients. Electrode-skin impedances were kept below 20 kΩ. EEG was continuously recorded for 30 min at a sampling rate of 1 kHz and band-pass filter of 0.1–100 Hz, with the vertex electrode as reference. The EEG was analysed using a semi-automatic procedure, which is illustrated in Fig. 1 and described below.

Electric source imaging method

Selection of interictal epileptogenic discharges and averaging

The offline analysis started with the visual selection of artefact-free interictal epileptogenic discharges by one of the authors (V.B.) experienced in reading clinical EEG and blinded to the patient history. The interictal epileptogenic discharges thus identified were compared with the results of the unblinded review by M.S. or S.V., who were in charge of the patient, and disagreement was resolved through discussion. In only very few patients, there was a discrepancy in the judgement (3/152; 1.9%).

In all patients, the standard EEG (low-resolution EEG) was available first and reviewed in order to determine the epileptogenic contacts with the most prevalent interictal epileptogenic discharges (i.e. >70%). In order to facilitate the recognition of the interictal discharges, the high-resolution EEG was reviewed in a simplified montage, and if interictal epileptogenic discharges were found, marked within the full montage.

Based on a report of the commission of terminology (Chatrian, 1974), the selection criteria were as follows: (i) paroxysmal occurrence; (ii) abrupt change in polarity; (iii) duration <200 ms; and (iv) the interictal discharge has a physiological field. While the Committee on Terminology differs between spikes (<70 ms) and sharp waves (<200 ms), we agree with Walczak and colleagues (2008) that the clinical utility of this differentiation is uncertain, in particular, in the present context. Deep sources may well present 'only' with sharp waves, which is due to the mixture of epileptogenic and overlying physiological electrical currents. Spikes and sharp waves are referred to as interictal epileptogenic discharges.

The interictal epileptogenic discharges were marked at the exact time point of maximal negativity on the electrode trace that showed highest amplitude. Only isolated interictal epileptogenic discharges were included in the analysis (i.e. without any other discharges within ±500 ms) and only the most dominant interictal epileptogenic discharge type was selected. All interictal epileptogenic discharges in a given patient had similar morphology and topography. Interictal epileptogenic discharges were then aligned to the global field power peak and averaged over epochs of ±500 ms around this peak. The EEG map at the 50% rising phase of the averaged interictal epileptogenic discharges was selected and subjected to the source localization procedure because it has been shown that the primary focus is most reliably localized during the rising phase of the interictal epileptogenic discharge, while the interictal epileptogenic discharge peak already involves areas of propagation (Lantz *et al.*, 2003; Ray *et al.*, 2007). All EEG analysis was carried out using the freely available software Cartool (Brunet *et al.*, 2011; https://sites.google.com/site/fbmlab/cartool).

Source localization

Source estimation was performed using the linear distributed inverse solution known as LAURA (local autoregressive average; Grave de Peralta *et al.*, 2004; Michel *et al.*, 2004). This source model is based on the physical law that the strength of a source regularly regresses with distance. Using a regular grid of solution points, the method incorporates this law in terms of a local autoregressive average with coefficients depending on the distance between solution points.

Head model

We used a simplified realistic head model to calculate the forward solution in which the anatomical head shape is taken into account and the solution space is constrained to the grey matter subspace within the volume conductor (SMAC model; Spinelli *et al.*, 2000). More concretely, the brain surface is extracted from the MRI and the best fitting sphere for this surface is calculated. Then the source space is warped according to the ratio of the sphere radius and the real surface radius. Around 3000 solution points are distributed with equal distances in the grey matter of this wrapped space. Because of this slight deformation of the brain to a best-fitting sphere, the lead field matrix could be computed using the known analytical solutions for a three-shell spherical head model (Ary *et al.*, 1981). These lead field matrices were then incorporated in the linear inverse solution algorithm LAURA described above. Finally, the result was back-transformed to the original head shape using the same transformation parameter. In order to evaluate the difference between the individual MRI and an average template MRI (see below), we calculated the SMAC head model for each individual MRI as well as for the averaged template MRI of the Montreal Neurological Institute (MNI) brain. In the case of the individual MRI, the individual anatomy was respected and altered cerebral structures were accounted for. The SMAC head model method has been successfully used in several previous clinical and experimental studies (e.g. Michel *et al.*, 2004; Phillips *et al.*, 2005; Brodbeck *et al.*, 2009, 2010; Groening *et al.*, 2009; Vulliemoz *et al.*, 2009, 2010; Siniatchkin *et al.*, 2010) and produces localization precisions that are comparable with realistic boundary element models (Guggisberg *et al.*, 2011).

Magnetic resonance imaging

All patients had MRI scans as part of the pre-surgical evaluation. They were acquired either with a 1.5 T Eclipse scanner (Picker Inc.) or a 3T Trio scanner (Siemens). The MRI was performed according to a standardized epilepsy protocol: coronal T_2-weighted fast spin-echo; repetition time 3092; echo time 11/100; voxel size $0.9 \times 0.9 \times 9.6$ mm, coronal and axial fluid-attenuated inversion recovery (FLAIR; repetition time 11 000; echo time 140; inversion time 2800; voxel size $0.45 \times 0.45 \times 6$ mm), sagittal 3D gradient echo T_1 (repetition time 12; echo time 4; voxel size 0.98×0.98 mm^2; thickness 1 mm) and diffusion sequences.

In 142 patients, the structural MRI showed a pathological result indicating an epileptogenic lesion; the other 10 patients had a normal MRI (five of the latter with temporal lobe epilepsy; Table 3).

Table 3 MRI findings

MRI finding	n
Normal	10
Abnormal	142
Hippocampal sclerosis (Hippocampal sclerosis alone/ Hippocampal sclerosis + ipsilateral anterior temporal lobe atrophy or other pathology)	53 (33/20)
Arteriorvenous malformation, cavernoma	13
Gliosis and focal atrophy	21
Neuronal migration disorder	
Dysplasia	18
DNET, ganglioglioma	19
Tuberous sclerosis	8
Lisencephaly/schizencephaly/heterotopia/ Sturge–Weber Syndrome	4
Other	
Porencephalic cysts	6

DNAT = dysembryoplastic neuroepithelial tumour.

In 29 patients, MRI showed multi-focal abnormalities. Both patients with normal MRI and multifocal lesions were considered together as 'non-focal'.

Positron emission tomography and single-photon emission-computed tomography acquisition

Fluorodeoxyglucose PET was carried out using 2-[^{18}F]fluoro-2-deoxy-D-glucose in all but one patient. Areas with focally decreased fluorodeoxyglucose uptake were identified by visual analysis.

For the ictal and interictal SPECT, a single bolus of 740 MBq of ethlenecysteinate dimer labelled with technetium-99 m ([^{99m}Tc] ethlenecysteinate dimer) was injected. SPECT scans were obtained 20–60 min after injection on a three-head Toshiba CGA-9300 camera. Only patients with an ictal exam were considered for analysis, verified by review of video-EEG recording. A total of 127 patients underwent ictal and interictal SPECT. Focus localization was determined by visual analysis and comparison of the ictal and interictal exam. In 70% of the patients, visual analysis was completed by subtraction analysis (SISCOM). From this point on, we will refer to both ictal and interictal SPECT with or without SISCOM analysis as 'ictal SPECT'.

Surgery

Patients underwent temporal or extratemporal surgical intervention considered appropriate for their needs. Each case was discussed in our weekly interdisciplinary case conference. Patients had left ($n = 71$) or right ($n = 81$) hemispheric resections. Temporal lobe surgery included all patients with a resection of temporal structures ($n = 102$), i.e. mesial temporal structures and to a variable degree anterior and/or lateral temporal neocortex. As in the patients with extratemporal lobe epilepsy ($n = 50$), resection was tailored and based on EEG, neuroimaging, analysis of ictal semiology and neuropsychological results. In the whole group, 31 patients had unilobar resections and 19 patients underwent multilobar resections.

All patients were seen postoperatively by the neurosurgeon and neurologist or neuropaediatrician. Mean follow-up was 4 years, 10 months (standard deviation: ± 2 years 10 months, median 5 years 3 months). Surgical outcome was measured at the latest visit.

Sensitivity and specificity evaluation

To evaluate the effect of the underlying brain template, we compared localization precision using the individual MRI and the averaged template MRI of the MNI as SMAC-transformed head model for the forward solution (see above).

In addition, we evaluated the effect of the number of electrodes on localization precision, i.e. comparing electric source imaging based on 64–256 EEG recordings (high-resolution electric source imaging) with those of standard EEG channel number (19–29 channels; low-resolution electric source imaging). This led to four constellations: low-resolution electric source imaging with template MRI, low-resolution electric source imaging with individual MRI, high-resolution electric source imaging with template MRI and high-resolution electric source imaging with individual MRI.

We considered seizure freedom following the operation to be the so-called 'ground truth'—unambiguous proof of correct localization of the epileptogenic focus. Sensitivity was defined as the percentage of patients with focus localization within the resected zone of all patients who were seizure-free ($n = 117$). We also computed this analysis for the Classes I and II patients together ($n = 133$). Specificity is defined as the percentage of patients with focus localization outside the resected zone in those patients who had an Engel Class III or IV outcome after surgery ($n = 19$).

We also determined the positive and negative predictive value. The positive predictive value represents the probability of becoming seizure-free when the source maximum was resected, and the negative predictive value represents the probability of continuing to have seizures if the electric source imaging focus was not resected. Since not all patients underwent high-resolution EEG, we performed a separate statistical analysis with those patients in whom high-resolution electric source imaging recordings were available (Tables 4 and 5). We used chi-square tests to assess the statistical significance of the difference of localization accuracy between the different constellations for the electric source imaging. A $P < 0.05$ was considered significant. In order to better appreciate the yield for temporal and extratemporal lobe epilepsies, we also performed a separate analysis for both patients groups.

Results

Yield of low versus high number of scalp electrodes for electric source imaging

Table 4 summarizes the overall sensitivity, specificity, positive and negative predictive values for all possible constellations of

Table 4 Comparative values of different constellations of low-resolution electric source imaging, high-resolution electric source imaging, individual MRI, template MRI in the whole population and in the 52 patients who received all four electric source imaging variants

Measure	LR-ESI/t-MRI (%)		LR-ESI/i-MRI		HR-ESI/t-MRI		HR-ESI/i-MRI
	$n = 152$	$n = 52$	$n = 98$	$n = 52$	$n = 55$	$n = 52$	$n = 52$
Sensitivity	55.6	59.1	65.9	72.7	76.1	75.0	84.1
Specificity	58.8	62.5	53.8	75.0	55.6	62.5	87.5
PPV	92.6	89.7	91.8	94.1	89.7	91.7	97.4
NPV	15.5	21.7	28.1	33.3	31.3	31.3	50.0

The left column values are based on the total number of patients. The right column values are based on the 52 patients that had received high resolution electric source imaging/individual MRI.
HR-ESI = high resolution electric source imaging based on 128–256 channel EEG recordings; i-MRI = patient's individual MRI; LR-ESI = low resolution electric source imaging based on 19–29 channel EEG recordings; t-MRI = template MRI;. NPV = negative predictive value; PPV = positive predictive value.

Table 5 Sensitivity, specificity, positive predictive value and negative predictive value of structural MRI, PET, SPECT and high resolution electric source imaging/individual MRI

Measure	MRI (%)		PET (%)		SPECT (%)		HR-ESI/i-MRI (%)
	n = 152	*n* = 52	*n* = 147	*n* = 51	*n* = 119	*n* = 43	*n* = 52
Sensitivity	76.3	72.7	68.7	65.1	57.7	54.3	84.1
Specificity	52.9	50.0	43.8	37.5	46.7	62.5	87.5
PPV	94.5	94.1	93.8	93.3	88.2	86.4	97.4
NPV	25.6	33.3	19.6	28.6	13.7	23.8	50.0

The left column values are based on the total number of patients. The right column values are based on the 52 patients that had high-resolution electric source imaging/individual MRI.

HR-ESI/i-MRI = high-resolution electric source imaging/individual MRI based on 128–256 channel EEG recordings and individual MRI; NPV = negative predictive value; PPV = positive predictive value.
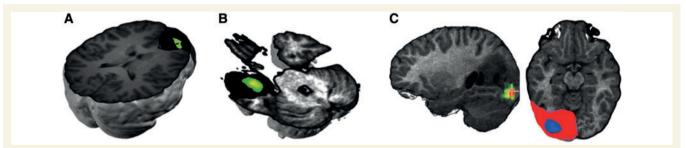

Figure 2 Examples of correct EEG source localization in operated and seizure-free patients. (**A**) Thirty-five-year-old patient with right frontal epilepsy and normal MRI. After subdural recordings, a polar frontal lobectomy was performed, which rendered the patient seizure-free. Histopathology revealed cortical dysplasia and gliosis. The green spot indicates the source maximum, which is superimposed on the postoperative MRI with the resected area marked in black. (**B**) Twenty-two-year-old patient with temporal lobe epilepsy and normal MRI. After depth recordings a left anterior temporal lobectomy was performed. Histopathology showed gliotic changes. The source maximum (green) was found within the resected area indicated in black. (**C**) Six-year-old female with a left occipital cystic lesion due to a ganglioglioma. A partial parieto-occipital lobectomy rendered the patient seizure-free. The source maximum was found in the occipital perilesional space (green) and lay within the resected area (indicated as blue spot in the red area that marks the resected zone).

low- and high-resolution electric source imaging and template and individual MRI for the patients who benefitted from surgery (Engel Classes I and II) versus those who did not (Engel Classes III and IV). The highest sensitivity (84.1%) and specificity (87.5%) were obtained with high-resolution electric source imaging using the patient's individual MRI as the head model (Fig. 4). Lowest values were obtained with low-resolution electric source imaging and template MRI (55.6 and 58.8%, respectively), followed by low-resolution electric source imaging/individual MRI and high-resolution electric source imaging/template MRI.

Considering only the 52 patients who underwent high-resolution electric source imaging and where an individual MRI was available, similar values were obtained (Table 4). If only patients with complete seizure freedom were analysed (Engel I), the sensitivities were as follows: low-resolution electric source imaging/template MRI 59.5%, low-resolution electric source imaging/individual MRI 70.8%, high-resolution electric source imaging/template MRI 81.6% and high-resolution electric source imaging/individual MRI 86.1% (Figs 2 and 3).

The statistical evaluation of the yield of high-resolution EEG and individual MRI was performed with the 43 patients for whom all imaging (i.e. including ictal SPECT) were available. This analysis revealed significant differences between both the high-resolution electric source imaging–individual MRI
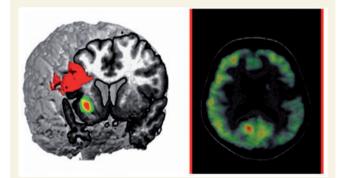

Figure 3 Example of a patient who was not seizure-free after operation; an 18-year-old patient with a surgical intervention in the right frontal posterior area (indicated in red) as suggested by intracranial recordings. The patient continued to have seizures after surgery. The electric source imaging source (green) showed a right insular maximum, which was concordant with a local hypometabolism found in the PET (*right*).

versus the low-resolution electric source imaging–individual MRI (*P* < 0.004), and the high-resolution electric source imaging–individual MRI versus the high-resolution electric source imaging-template MRI (*P* < 0.002).
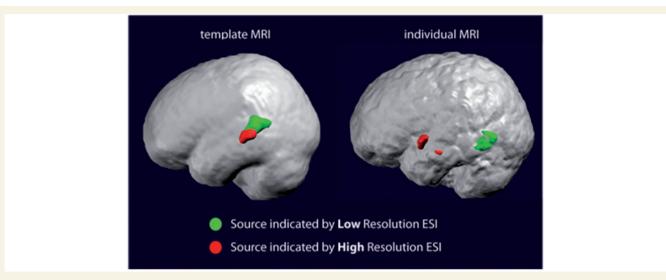
Figure 4 Example of a patient with non-concordant results between high- and low-resolution electric source imaging. Solutions using a template MRI are shown on the *left*, with the individual MRI on the *right*, low-resolution electric source imaging source superposed in green and high-resolution electric source imaging in red. The patient is a 13-year-old male with Engel Class II outcome after resection of the left temporal lobe. Only high-resolution electric source imaging based on the individual MRI correctly indicated a left anterior temporal source. Low- and high-resolution electric source imaging based on the template MRI indicated a parietal source.
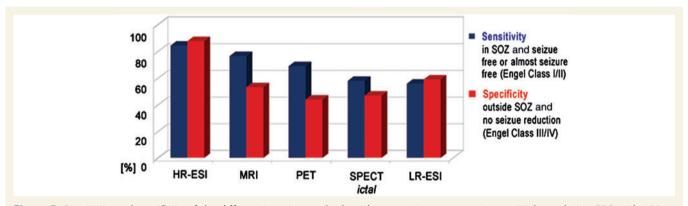

Figure 5 Sensitivity and specificity of the different imaging methods with respect to surgery outcome. High-resolution EEG with 128 or 256 electrodes had highest sensitivity (correct localization in seizure-free or almost seizure-free patients, Engel Classes I and II) and highest specificity (not localized in the resected zone in patients and without major benefit from surgery, Engel Classes III and IV). HR-ESI = high-resolution electric source imaging; LR-ESI = low-resolution electric source imaging; SOZ = seizure onset zone.

Comparison of high-resolution electric source imaging/individual MRI with the established structural and functional imaging techniques

Almost all patients had a PET exam ($n = 147$). Ictal SPECT was obtained from 119 (79%) patients. Compared with high-resolution electric source imaging (using individual MRI) the structural MRI alone provided slightly lower sensitivity (76.3% versus 84.1%) and markedly lower specificity (52.9% versus 87.5%), followed by PET (sensitivity 68.7%, specificity 43.8%) and ictal SPECT (sensitivity 57.7%, specificity 46.7%; Table 5 and Fig. 5). In the group of 43 patients, who had all imaging exams (35 Engel Classes I + II, eight Engel Classes III + IV), similar sensitivities and

specificities were obtained as with the entire patient group (sensitivity: high-resolution electric source imaging/individual MRI 80%, MRI 71.4%, PET 62.9%, ictal SPECT 54.3%, specificity: high-resolution electric source imaging/individual MRI 88%, MRI 50%, PET 37.5%, ictal SPECT 62.5). The details of the results of all 152 patients are given in Supplementary Table 1.

Comparison of patients with temporal versus extratemporal lobe epilepsy

In order to determine the relative yield of electric source imaging for patients with temporal and extratemporal lobe epilepsies, sensitivities and specificities were calculated for all electrical source imaging constellations and imaging exams separately for

Table 6 Comparison of sensitivity of all electric source imaging constellations separately for cases with temporal and extratemporal lobe epilepsy

Group	LR-ESI/t-MRI, n (%)	LR-ESI/i-MRI, n (%)	HR-ESI/t-MRI, n (%)	HR-ESI/i-MRI, n (%)
TLE	102 (57.3)	56 (67.3)	n = 26 (100)	n = 25 (91.7)
ETLE	50 (51.3)	42 (63.6)	29 (76.2)	27 (75.0)

ETLE = extratemporal lobe epilepsy; HR-ESI = high-resolution electric source imaging based on 128–256 channel EEG recordings; LR-ESI = low-resolution electric source imaging based on 19–29 channel EEG recordings; TLE = temporal lobe epilepsy.

Table 7 Comparison of sensitivity of all imaging exams in those patients who underwent high resolution electric source imaging/individual MRI and the other imaging exams

Group	HR-ESI/i-MRI, n (%)	MRI, n (%)	PET, n (%)	Ictal SPECT, n (%)
TLE	25 (91.7)	25 (70.8)	24 (69.6)	19 (61.1)
ETLE	27 (75.0)	27 (75.0)	27 (60.0)	24 (47.1)

ETLE = extratemporal lobe epilepsy; HR-ESI = high-resolution electric source imaging based on 128–256 channel EEG recordings; LR-ESI = low-resolution electric source imaging based on 19–29 channel EEG recordings; TLE = temporal lobe epilepsy.
Due to too small numbers of the negative cases, only sensitivity values are given.

both patient groups. Due to the small number of negative cases in the subgroups, the calculation of specificity, positive and negative predictive values was not meaningful. Again, highest sensitivity values were obtained for high-resolution electric source imaging/ individual MRI, somewhat higher for temporal than for extratemporal lobe epilepsy. However, the difference was not significant (Table 6). In the group of 25 patients with temporal lobe epilepsy and 27 patients with extratemporal lobe epilepsy, respectively, who had high-resolution electric source imaging/individual MRI, again this imaging technique compares favourably to the other imaging exams, providing the highest sensitivity values (Table 7).

Discussion

Pre-surgical evaluation usually requires a comprehensive—and often costly—battery of brain imaging tools, to obtain precise localizing information regarding the epileptogenic focus. Only after the focus is completely removed, will the patient have a realistic chance of postoperative seizure freedom, which is still difficult to obtain with patients without magnetic resonance lesion and/or extratemporal lobe epilepsy. The current study was undertaken to determine the overall yield of electric source imaging prospectively in a large patient population referred for evaluation of pharmacoresistant epilepsy. Our gold standard was seizure freedom after operation, as used in many electric source imaging, magnetic source imaging and EEG–functional MRI studies

(e.g. Thornton *et al.*, 2010; Grouiller *et al.* 2011; Seo *et al.*, 2011). If electric source imaging of interictal discharges were localized within the resected volume, the solution was considered correct. The same criterion was used for the other imaging methods as well. It is the level of precision that is clinically relevant in the presurgical evaluation.

In our series of 152 patients with epilepsy, electric source imaging based on high-resolution EEG (mostly with 128 or 256 electrodes), and with the patient's own MRI as the head model, provided excellent localization precision with a sensitivity of 84% and specificity of 88%. When only standard EEG was available for electric source imaging (low resolution), a sensitivity of 66% was obtained, when ESI was based on the individual MRI. Not unexpectedly, lowest sensitivity and specificity were obtained when using only standard EEG and a template MRI. Thus, if the epileptogenic zone was identified with high-resolution electric source imaging/individual MRI, the chances that the focus was indeed at this site were 84%. We also had a few failure cases and in-depth analysis revealed that in most of them, propagated interictal epileptiform discharges (to the ipsilateral anteromesial temporal lobe) were used for electric source imaging, given that they were the only clearly visible epileptogenic anomalies. The true foci, at distance, of the electric source imaging focus were characterized by low-amplitude rapid rhythms, seen in the intracranial ictal and interictal EEG. The excellent localizing value of high-frequency oscillations (Urrestarazu *et al.*, 2007; Worrell *et al.*, 2008) or high-frequency interictal discharges (McGonigal *et al.*, 2007) is well established. In order to improve the sensitivity of high-resolution electric source imaging even further, the visualization of these β- or γ-rhythms in the scalp EEG would be mandatory, which, however, is difficult in light of the small size of signals and possible muscle artefacts contamination.

The present study confirms previous studies on electric source imaging in epilepsy with smaller numbers of patients. In a group of 32 patients (Michel *et al.*, 2004b), correct localization on a lobar level was obtained in 93.7% with electric source imaging based on 128 channel EEG. Sperli and colleagues (2006) analysed the standard clinical EEG with electric source imaging of 30 operated and seizure-free children, using mostly 29 electrodes and the patients' MRI (i.e. low-resolution electric source imaging/individual MRI). They reported correct localization on a lobar level in 90% of the cases. However, correct localization at a lobar level does not necessarily mean that the source maximum was within the resected zone, which was the criterion in the current study. In the study by Michel and colleagues (2004b), this criterion was applied in the 24 operated patients. In this case, correct localization was found in 79% using high-resolution electric source imaging/individual MRI, which is comparable with the current result with a larger number of patients.

Electric source imaging is a particularly valuable tool for analysing patients with normal MRI. Brodbeck and colleagues (2010) analysed 10 operated patients in whom modern MRI sequences failed to provide evidence of an epileptogenic (temporal and extratemporal) lesion. Nevertheless, electric source imaging showed correct focus localization in eight of them. Thus, even in this particularly difficult patient group where the MRI provides no relevant information, electric source imaging helped clinicians

to determine the epileptogenic focus in the individual brain with excellent precision.

This study does not include a comparison with MEG recordings because it is not a typical part of the pre-surgical work-up at the University Hospital in Geneva, and thus the issue of whether it can make a cost-effective contribution to the localization of the epileptic focus is not addressed in the present publication. Some key issues that deserve attention in future studies that do look at MEG potential contribution include the ongoing discussion about how deeply EEG and MEG can 'see'. There are concerns that MEG may miss deep sources and that it is insensitive to sources with radial orientation (Ahlfors et al., 2010), which appears to be less of an issue in EEG (Lejten et al., 2003).

Another debate concerns the possibility to localize mesial temporal interictal epileptiform discharges through inverse solutions. Several studies suggest that anterior temporal spikes recorded on the scalp are rather the result of anterior or lateral neocortical temporal activity or common activity of neocortical and mesial temporal sources, and that neither EEG nor MEG can see spikes confined to the mesial temporal structures (Alarcon et al., 1994; Emerson et al., 1995; Huppertz et al., 2001; Gavaret et al., 2004; Wennberg 2011). However, simultaneous surface and intracranial EEG studies indicated that deep mesial temporal sources could be properly localized by electric source imaging if their small volume-conducted signals can be identified in the scalp EEG, or if they are averaged (Lantz et al., 2001; Nayak et al., 2004; Zumsteg et al., 2005; Nahum et al., 2011). It remains to be shown in future studies using simultaneous intracranial EEG if mesial temporal interictal epileptiform discharges could be localized non-invasively with high-density EEG/MEG or with combined EEG–functional MRI (Sperli et al., 2006; Kaiboriboon et al., 2010; Vulliemoz et al., 2010; Grouiller et al., 2011).

Another potential concern regarding the use of electric source imaging for pre-surgical epilepsy evaluation is that it is done using 'interictal discharges' instead of 'ictal recordings', which are supposedly more relevant when deciding where to operate. However, the scalp EEG studies cited earlier, as well as studies from patients with intracranial electrodes, strongly suggest that careful analysis of the localization of interictal epileptiform discharges, or the majority of interictal epileptiform discharges, allow a good-to-excellent estimate of the ictal source (Asano et al., 2003; Ray et al., 2007). It is important to note that electric source imaging is not restricted to interictal activity as is MEG or functional MRI, because EEG can be recorded over a much longer duration and motion does not make the recordings invalid. Recent studies have shown successful localization of the seizure onset zone with electric source imaging, extending its use to ictal long-term recordings with up to 256 electrodes (Holmes et al., 2008; Stern et al., 2009).

The optimal mathematical approach for the analysis of EEG (or MEG) data for source localization has been addressed in numerous publications and it is beyond the scope of the present publication to go into details. While simple equivalent dipole fitting provides good source estimations (Gavaret et al., 2009; Rose and Ebersole, 2009), a crucial step towards achieving a real 3D imaging of the electrical activity in the brain was obtained by distributed inverse solution algorithms that are able to visualize the current density distribution in the entire brain at each moment in time (for reviews see Michel et al., 2004a; Plummer et al., 2008). With these 3D algorithms, the electric source can be identified in most of the patients, even in the presence of large, inhomogeneous lesions (Brodbeck et al., 2009).

Our results from this large patient group show that electric source imaging based on large electrode arrays covering the whole skull is an excellent tool to localize the epileptogenic focus, with excellent sensitivity and specificity. However, until recently, the lack of 'adoption' of EEG-based electric source imaging in the clinical world has mainly been because the application of a high number of electrodes (i.e. between 100 and 200 or even more) was too cumbersome to perform routinely. Due to technical progress, electric source imaging using large-array recordings can be obtained in <30 min and does not require highly experienced, well-trained personnel, expensive shielding or other inconveniences. Commercially available high-resolution EEG systems make recordings from a large number of electrodes fast and easy, and they even integrate with MRI data.

Our source analysis was based on a simplified head model that allowed a fast and analytical solution of the forward problem. More realistic head models based on boundary or finite element meshing of the brain are nowadays available in some software packages and will soon be feasible in daily clinical applications (Michel and He, 2011). There is little doubt that these more realistic head models will further increase the accuracy of electric source imaging, particularly if inhomogeneous conductivities of the brain and orientation constraints of the dipoles are incorporated. Most importantly, however, is the use of the individual MRI of the patient instead of a template MRI, as shown in the current study as well as in a recent study by Guggisberg et al. (2011). For almost all patients with epilepsy admitted for surgery, high-resolution MRI is usually available and is easily integrated into the analysis.

From a practical clinical perspective, electric source imaging on the basis of high-resolution EEG (i.e. with 128–256 scalp electrodes) is very interesting. The sensitivity and specificity of electric source imaging is as high as (or even higher than) more established brain imaging techniques, and electric source imaging is relatively inexpensive when compared with nuclear medicine techniques or MRI-based approaches. Moreover, the electric source imaging exam does not require sedation, which considerably reduces the workload for working with children or mentally retarded persons, who are unable to remain immobile for 30 min or more. The more precise focus localization of electric source imaging also allows better preparation for intracranial electrode implantations if deemed necessary (Seeck et al. 2010).

Acknowledgements

Funding

Supplementary material

Supplementary material is available at *Brain* online.

References

Ahlfors SP, Han J, Belliveau JW, Hamalainen MS. Sensitivity of MEG and EEG to source orientation. Brain Topogr 2010; 23: 227–32.

Alarcon G, Guy CN, Binnie CD, Walker SR, Elwes RD, Polkey CE. Intracerebral propagation of interictal activity in partial epilepsy: implications for source localisation. J Neurol Neurosurg Psychiatry 1994; 57: 435–49.

Ary JP, Klein SA, Fender DH. Location of sources of evoked scalp potentials: Corrections for skull and scalp thicknesses. IEEE Trans Biomed Eng 1981; 28: 834–6.

Asano E, Muzik O, Shah A, Juhasz C, Chugani DC, Sood S, et al. Quantitative interictal subdural EEG analyses in children with neocortical epilepsy. Epilepsia 2003; 44: 425–34.

Brodbeck V, Lascano AM, Spinelli L, Seeck M, Michel CM. Accuracy of EEG source imaging of epileptic spikes in patients with large brain lesions. Clin Neurophysiol 2009; 120: 679–85.

Brodbeck V, Spinelli L, Lascano AM, Pollo C, Schaller K, Vargas MI, et al. Electrical source imaging for presurgical focus localization in epilepsy patients with normal MRI. Epilepsia 2010; 51: 583–91.

Brunet D, Murray MM, Michel CM. Spatiotemporal analysis of multichannel EEG: CARTOOL. Comput Intell Neurosci 2011; 2011, doi:10.1155/2011/813870.

Chatrian GE. Report on the Committee on Terminology. Proceedings of the General Assembly. The VIIIth International £Congress of Electroencephalography and Clinical Neurophysiology. Electroencephalogr Clin Neurophysiol 1974; 37: 521–53.

Emerson RG, Turner CA, Pedley TA, Walczak TS, Forgione M. Propagation patterns of temporal spikes. Electroencephalogr Clin Neurophysiol 1995; 94: 338–48.

Fuchs M, Wagner M, Kastner J. Development of volume conductor and source models to localize epileptic foci. J Clin Neurophysiol 2007; 24: 101–19.

Gavaret M, Badier JM, Marquis P, Bartolomei F, Chauvel P. Electric source imaging in temporal lobe epilepsy. J Clin Neurophysiol 2004; 21: 267–82.

Gavaret M, Trebuchon A, Bartolomei F, Marquis P, McGonigal A, Wendling F, et al. Source localization of scalp-EEG interictal spikes in posterior cortex epilepsies investigated by HR-EEG and SEEG. Epilepsia 2009; 50: 276–89.

Grave de Peralta Menendez R, Murray MM, Michel CM, Martuzzi R, Gonzalez Andino SL. Electrical neuroimaging based on biophysical constraints. Neuroimage 2004; 21: 527–39.

Groening K, Brodbeck V, Moeller F, Wolff S, van Baalen A, Michel CM, et al. Combination of EEG-fMRI and EEG source analysis improves interpretation of spike-associated activation networks in paediatric pharmacoresistant focal epilepsies. Neuroimage 2009; 46: 827–33.

Grouiller F, Thornton RC, Groening K, Spinelli L, Duncan JS, Schaller K, et al. With or without spikes: localization of focal epileptic activity by simultaneous electroencephalography and functional magnetic resonance imaging. Brain 2011; 134: 2867–86.

Guggisberg AG, Dalal SS, Zumer JM, Wong DD, Dubovik S, Michel CM, et al. Localization of cortico-peripheral coherence with electroencephalography. Neuroimage 2011; 57: 1348–57.

Huppertz HJ, Hof E, Klisch J, Wagner M, Lücking CH, Kristeva-Feige R. Localization of interictal delta and epileptiform EEG activity associated with focal epileptogenic brain lesions. Neuroimage 2001; 13: 15–28.

Henry TR, Van Heertum RL. Positron emission tomography and single photon emission computed tomography in epilepsy care. Semin Nucl Med 2003; 33: 88–104.

Holmes MD, Tucker DM, Quiring JM, Hakimian S, Miller JW, Ojemann JG. Comparing noninvasive dense array and intracranial electroencephalography for localization of seizures. Neurosurgery 2008; 66: 354–62.

Kaiboriboon K, Nagarajan S, Mantle M, Kirsch HE. Interictal MEG/magnetic source imaging in intractable mesial temporal lobe epilepsy: spike yield and characterization. Clin Neurophysiol 2010; 121: 325–31.

Knowlton RC, Elgavish RA, Bartolucci A, Ojha B, Limdi N, Blount J, et al. Functional imaging: II. Prediction of epilepsy surgery outcome. Ann Neurol 2008; 64: 35–41.

Knowlton RC, Razdan SN, Limdi N, Elgavish RA, Killen J, Blount J, et al. Effect of epilepsy magnetic source imaging on intracranial electrode placement. Ann Neurol 2009; 65: 716–23.

Lantz G, Grave de Peralta Menendez R, Gonzalez Andino S, Michel CM. Noninvasive localization of electromagnetic epileptic activity. II. Demonstration of sublobar accuracy in patients with simultaneous surface and depth recordings. Brain Topogr 2001; 14: 139–47.

Lantz G, Spinelli L, Seeck M, de Peralta Menendez RG, Sottas CC, Michel CM. Propagation of interictal epileptiform activity can lead to erroneous source localizations: a 128-channel EEG mapping study. J Clin Neurophysiol 2003; 20: 311–9.

Leijten FS, Huiskamp GJ, Hilgersom I, Van Huffelen AC. High-resolution source imaging in mesiotemporal lobe epilepsy: a comparison between MEG and simultaneous EEG. J Clin Neurophysiol 2003; 20: 227–38.

Manford M, Fish DR, Shorvon SD. An analysis of clinical seizure patterns and their localizing value in frontal and temporal lobe epilepsies. Brain 1996; 119: 17–40.

McGonigal A, Bartolomei F, Régis J, Guye M, Gavaret M, Trébuchon-Da Fonseca A, et al. Stereoelectroencephalography in presurgical assessment of MRI-negative epilepsy. Brain 2007; 130: 3169–83.

Michel CM, He B. EEG Mapping and source imaging. In: Schomer D, Lopes da Silva F, editors. Niedermeyer's electroencephalography. 6th edn., Chapter 55. Lippincott Williams & Wilkins; 2011. p. 1179–202.

Michel CM, Lantz G, Spinelli L, De Peralta RG, Landis T, Seeck M. 128-channel EEG source imaging in epilepsy: clinical yield and localization precision. J Clin Neurophysiol 2004b; 21: 71–83.

Michel CM, Murray MM, Lantz G, Gonzalez S, Spinelli L, Grave de Peralta R. EEG source imaging. Clin Neurophysiol 2004a; 115: 2195–222.

Nahum L, Gabriel D, Spinelli L, Momjian S, Seeck M, Michel CM, et al. Rapid consolidation and the human hippocampus: Intracranial recordings confirm surface EEG. Hippocampus 2011; 21: 689–93.

Nayak D, Valentín A, Alarcón G, García Seoane JJ, Brunnhuber F, Juler J, et al. Characteristics of scalp electrical fields associated with deep medial temporal epileptiform discharges. Clin Neurophysiol 2004; 115: 1423–35.

Phillips C, Mattout J, Rugg MD, Maquet P, Friston KJ. An empirical Bayesian solution to the source reconstruction problem in EEG. Neuroimage 2005; 24: 997–1011.

Plummer C, Harvey AS, Cook M. EEG source localization in focal epilepsy: where are we now? Epilepsia 2008; 49: 201–18.

Ray A, Tao JX, Hawes-Ebersole SM, Ebersole JS. Localizing value of scalp EEG spikes: a simultaneous scalp and intracranial study. Clin Neurophysiol 2007; 118: 69–79.

Rose S, Ebersole JS. Advances in spike localization with EEG dipole modeling. Clin EEG Neurosci 2009; 40: 281–7.

Seo JH, Holland K, Rose D, Rozhkov L, Fujiwara H, Byars A, et al. Multimodality imaging in the surgical treatment of children with nonlesional epilepsy. Neurology 2011; 76: 41–8.

Seeck M, Schomer DL, Bergey GK, Niedermeyer E. Intracranial monitoring: depth, subdural and foramen ovale electrodes. In: Schomer DL,

Lopes da Silva F, editors. Niedermeyer's textbook of electroencephalography: basic principles, clinical applications, and related fields. VI edn., Chapter 33. Wolters Kluwer and Lippincott; 2010.

Siniatchkin M, Groening K, Moehring J, Moeller F, Boor R, Brodbeck V, et al. Neuronal networks in children with continuous spikes and waves during slow sleep. Brain 2010; 133: 2798–813.

Spanaki MV, Spencer SS, Corsi M, MacMullan J, Seibyl J, Zubal IG. Sensitivity and specificity of quantitative difference SPECT analysis in seizure localization. J Nucl Med 1999; 40: 730–6.

Sperli F, Spinelli L, Seeck M, Kurian M, Michel CM, Lantz G. EEG source imaging in pediatric epilepsy surgery: a new perspective in presurgical workup. Epilepsia 2006; 47: 981–90.

Spinelli L, Andino SG, Lantz G, Seeck M, Michel CM. Electromagnetic inverse solutions in anatomically constrained spherical head models. Brain Topogr 2000; 13: 115–25.

Stern Y, Neufeld MY, Kipervasser S, Zilberstein A, Fried I, Teicher M, et al. Source localization of temporal lobe epilepsy using PCA-LORETA analysis on ictal EEG recordings. J Clin Neurophysiol 2009; 26: 109–16.

Sutherling WW, Mamelak AN, Thyerlei D, Maleeva T, Minazad Y, Philpott L, et al. Influence of magnetic source imaging for planning intracranial EEG in epilepsy. Neurology 2008; 71: 990–6.

Thornton R, Laufs H, Rodionov R, Cannadathu S, Carmichael DW, Vulliemoz S, et al. EEG correlated functional MRI and postoperative outcome in focal epilepsy. J Neurol Neurosurg Psychiatry 2010; 81: 922–7.

Urrestarazu E, Chander R, Dubeau F, Gotman J. Interictal high-frequency oscillations (100-500 Hz) in the intracerebral EEG of epileptic patients. Brain 2007; 130: 2354–66.

Vergult A, De Clercq W, Palmini A, Vanrumste B, Dupont P, Van Huffel S, et al. Improving the interpretation of ictal scalp EEG: BSS-CCA algorithm for muscle artifact removal. Epilepsia 2007; 48: 950–8.

Vulliemoz S, Rodionov R, Carmichael DW, Thornton R, Guye M, Lhatoo SD, et al. Continuous EEG source imaging enhances analysis of EEG-fMRI in focal epilepsy. Neuroimage 2010; 49: 3219–29.

Vulliemoz S, Thornton R, Rodionov R, Carmichael DW, Guye M, Lhatoo S, et al. The spatio-temporal mapping of epileptic networks: combination of EEG-fMRI and EEG source imaging. Neuroimage 2009; 46: 834–43.

Walczak TS, Jayakar P, Mizrahi EM. Interictal encephalography. In: Engel J Jr, Pedley TA, editors. Epilepsy – a comprehensive textbook. 2nd edn. Wolters-Kluwer Lippincott Williams & Wilkins; 2008. p. 809–823.

Wennberg R, Valiante T, Cheyne D. EEG and MEG in mesial temporal lobe epilepsy: where do the spikes really come from? Clin Neurophysiol 2011; 122: 1295–313.

Worrell GA, Gardner AB, Stead SM, Hu S, Goerss S, Cascino GJ, et al. High-frequency oscillations in human temporal lobe: simultaneous microwire and clinical macroelectrode recordings. Brain 2008; 13: 928–37.

Zumsteg D, Friedman A, Wennberg RA, Wieser HG. Source localization of mesial temporal interictal epileptiform discharges: correlation with intracranial foramen ovale electrode recordings. Clin Neurophysiol 2005; 116: 2810–8.

Zumsteg D, Friedman A, Wieser HG, Wennberg RA. Source localization of interictal epileptiform discharges: comparison of three different techniques to improve signal to noise ratio. Clin Neurophysiol 2006; 117: 562–71.